Electromagnetic particle injector for fast time response disruption mitigation in tokamaks

Electromagnetic particle injector for fast time response disruption mitigation in tokamaks

R. Raman[1], **W.-S. Lay**[1], **T.R. Jarboe**[1], **J.E. Menard**[2] and **M. Ono**[2]

[1] University of Washington, Seattle, WA, United States of America
[2] Princeton Plasma Physics Laboratory, Princeton, NJ, United States of America

E-mail: raman@aa.washington.edu

Abstract

A novel, rapid time-response, disruption mitigation system referred to as the electromagnetic particle injector (EPI) is described. This method can accurately deliver the radiative payload to the plasma center on a <10 ms time scale, much faster, and deeper, than what can be achieved using conventional methods. The EPI system accelerates a sabot electromagnetically. The sabot is a metallic capsule that can be accelerated to desired velocities by an electromagnetic impeller. At the end of its acceleration, within 2 ms, the sabot will release a radiative payload, which is composed of low-z granules, or a shell pellet containing smaller pellets. The primary advantage of the EPI concept over gas propelled systems is its potential to meet short warning time scales, while accurately delivering the required particle size and materials at the velocities needed for achieving the required penetration depth in high power ITER-scale discharges for thermal and runaway current disruption mitigation. The present experimental tests from a prototype system have demonstrated the acceleration of a 3.2 g sabot to over 150 m s^{-1} within 1.5 ms, consistent with the calculations, giving some degree of confidence that larger ITER-scale injector can be developed.

Keywords: EPI, DMS, disruption, particle injector, electromagnetic

(Some figures may appear in colour only in the online journal)

1. Introduction

Predicting and controlling disruptions is an important and urgent issue for ITER. Because tokamaks rely on a large amount of plasma current to generate the plasma equilibrium, there exists the possibility that Magnetohydrodynamic (MHD) instability of this current channel or that of the overall plasma equilibrium could be rapidly lost resulting in a major plasma disruption. A major plasma disruption in ITER or a tokamak-based reactor facility with a very high plasma stored energy would result in undesirable machine downtime and possibly expensive repairs to the reactor vessel and internal components. Thus, methods to safely quench the plasma discharge after an impending disruption detection are essential to protect the next generation tokamaks such as ITER and future tokamak reactors. As stated in [1], the thermal quench (TQ) onset time, from disruption mitigation system (DMS) trigger to plasma TQ, is desired to be faster than 20 ms, ideally, 10 ms, which poses stringent requirements on the DMS for reactor systems. This paper describes a novel disruption mitigation method referred to as the electromagnetic particle injector (EPI) concept. The EPI system accelerates a sabot electromagnetically. The sabot is a metallic capsule that can be accelerated to high velocity by an electromagnetic impeller. At the end of its acceleration, within 2 ms, the sabot will release the radiative payload that is composed of granules of low-z materials, or a shell pellet containing smaller pellets. The system is fully electromagnetic, with no mechanical moving parts that needs to operate reliably over many cycles, which ensures high reliability after a period of long standby. The only moving components are the sabot, which is not reused, and the payload which is injected into the tokamak plasma.

1741-4326/19/016021+10$33.00

1

In an earlier paper [2], we described the results of a scoping study to examine the theoretical capability and feasibility of an EPI system for a fusion reactor. In this paper, we report experimental tests that have verified the most important advantages of the EPI concept, that of the rapid response time and the achievement of the predicted sabot velocities on this fast time scale, giving some degree of confidence that larger ITER-scale injector can be developed.

1.1. Limitations of conventional methods

MGI (massive gas injection) and shattered pellet injection (SPI) are the most developed methods for disruption mitigation thus far [3–8]. In the MGI method [9, 10] a fast acting gas valve empties a high-pressure plenum filled with a radiative payload gas into the tokamak discharge to initiate a controlled radiative collapse of the plasma discharge. Due to the presence of high neutron flux or due to other reasons such as the possibility of elevated ambient temperatures near the tokamak vessel, the valve needs to be located some distance away from the vessel [11]. This means at least several meters away from the plasma on ITER. The Shattered Pellet [12] injection system accelerates a cryogenic pellet composed of neon, argon, deuterium or some combination of these elements and relies on a high-pressure gas pulse from a MGI valve to propel the frozen pellet [13]. Prior to injection into the tokamak plasma, the pellet is fragmented, and smaller shards are injected into the plasma.

A limitation with the use of gases in the MGI system, or for pellet propulsion, whether they be solid refractory, shell, or cryogenic shatterable, is that the propellant gas limits the gas and pellet velocity, before fragmentation, to about 300–400 m s^{-1} [14]. Consequently, the projected response time for the MGI and SPI systems on ITER is over 30 ms [15]. Thus, for example, although few km s^{-1} velocities have been demonstrated by two-stage light gas guns [16], integrated operation of this system to demonstrate its fast-time response capability is needed for it to be considered for DMS applications.

Because of its simplicity, MGI systems will probably continue to be used in tokamaks, as they may find use as a secondary backup system that can easily inject large quantities of a radiative payload gas, but on a slower response timescale. Gas assimilation from MGI is a complicated process. As described by Leonov *et al*, in simulations examining the impurity gas assimilation by the JET plasma, gas assimilation by the plasma is not just determined by the gas flow velocity or the proximity of the gas injector to the plasma, but one that may be influenced by the plasma response itself [17]. The simulation results show that the energy loss during MGI initiated disruption mitigation (DM) takes place in two phases: First, the pre-Thermal Quench (pre-TQ) phase that lasts from the arrival of the first gas to the onset of increased transport due to MHD activity. This is followed by the second thermal quench phase when most of the energy is radiated. The TQ begins after a critical fraction of impurities is assimilated during the pre-TQ phase so that when the impurity content reaches an amount sufficient for radiative energy loss to overpower Joule

heating, the cooling front begins to propagate inward accompanied by plasma current contraction. The simulations further suggest that the pre-TQ duration is nearly independent of the D_2 influx, and is determined primarily by the accumulation of the radiating impurity. Increasing the plenum pressure or reducing the distance between the valve and plasma largely shortens the pre-TQ phase. Thus, it may not be possible to arbitrarily control the assimilated amount of radiative material using MGI. Nevertheless, the DMS must be designed such that the impurity amount assimilated by the plasma is sufficient for re-radiation of more than 90% of heat flux during the subsequent TQ phase of the disruption [18, 19].

In this regard, the SPI concept is much superior to the MGI system [20]. Because the SPI concept injects solid particles of frozen high-z gas, the radiative payload assimilation by the plasma should not be as severely constrained as the theoretical simulations for MGI would suggest, because, in principle, one could inject these particles deeper into the plasma even after a thermal quench initiates. Indeed, experiments on DIII-D have shown it to be much superior to MGI in all regards [1]. The capability of the present SPI systems, however, is severely restricted by the velocities that can be achieved by the shattered fragments. First, the initial attainable velocity of the un-fragmented SPI pellet decreases with the mass of the pellet [14]. Based on measurements for argon pellets (with an initial velocity of 156 m s^{-1}) and from measurements of deuterium pellets, the size distribution for the bulk of the fragment particles is about 1 mm [21]. Velocities, before fragmentation, of 200 m s^{-1} have been reported for neon SPI on DIII-D [22].

At higher velocities, the much higher kinetic energy of the pellet, upon impact with the target plate results in a larger fraction of the pellet vaporizing, and the solid fraction reduction. Under these conditions, the capability of the SPI system is diminished due to the undesirable contribution from the vaporized SPI fragments. Because of the energetic nature of high-powered tokamak discharges, 25 kPa pedestal pressure on DIII-D Super H-mode plasmas [23] and over 100 kPa anticipated on ITER, this combination of velocity and pellet size may pose severe challenges for attaining deep SPI fragment penetration in these much more energetic reactor-grade plasmas.

A new system being tested on DIII-D, referred to as the Shell Pellet [24] overcomes this issue of deep penetration into a high-power tokamak discharge. The shell pellet achieves this capability by encapsulating the radiative payload inside a thin-shell chamber (which could be solid low-z elements or a combination of low-z elements and pressurized high-z gas) and the entire pellet is injected into the plasma discharge. During propagation into the plasma, the shell would ablate in a manner so as to permit much of the radiative payload to be deposited deeper in the plasma, quite likely in the region where the runaway electron channel forms, thus possibly suppressing the formation of this current channel in the first place. At present this system however still suffers from slow response time and relatively low maximum attainable velocities as it relies on gas for propulsion as other gas-based concepts.
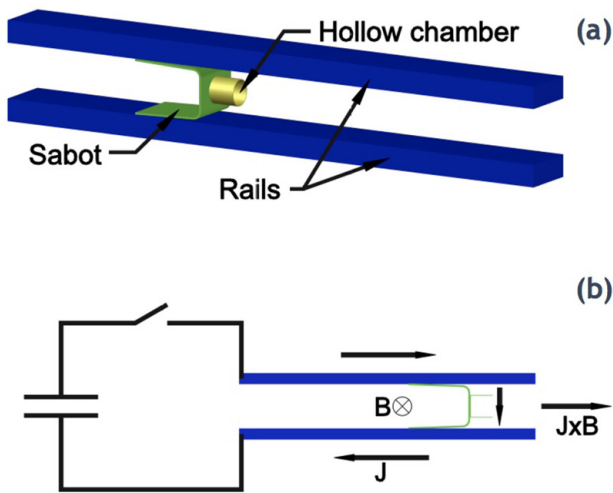
Figure 1. Simplified description of the EPI concept. (*a*) A metallic sabot with a hollow chamber to transport the payload is placed between two parallel metal rails. (*b*) Discharging a charged capacitor bank causes current to flow from one rail to the other through the sabot. The magnetic field generated inside the gap between the rails, due to the current in the rails, crossed with the current flowing in the sabot results in a $\mathbf{J} \times \mathbf{B}$ force that propels the sabot. Deploying magnetic field coils that are located above and or below the rails could add to the magnetic field in the sabot region, which would help reduce the rail current required to attain a given sabot velocity.

As will be described in the next section, the EPI system overcomes these difficulties; it shares some advantages of the shell pellet concept and it is also suitable for injecting some forms of shell pellets.

2. Advantages of the EPI system

The proposed EPI method could be used to accelerate any impurity pellets. For ITER, the preferred radiative payload would be microspheres of Be, BN or B. These materials were chosen based on discussions with ITER personnel listed under the Acknowledgments section. These materials are suitable for ITER as they do not chemically react with tritium.

In order for the microspheres to remain robustly inside the payload cavity, shown in figure 1, they either need be contained inside a thin shell capsule composed of Be, B or BN or the microspheres need to weakly bonded to each other so that they do not dribble out of the sabot cavity. Thus, it is not necessary for the thin shell to be strong enough to withstand the acceleration forces. However, it may also be possible to use a conventional shell pellet as described in [2], but the design of such a shell is something that could be investigated as the need arises. Others, such as Hollmann, are engaged in the development shell pellets [25]. An important advantage of the use of non-cryogenic materials is that the payload could remain in its initial state for long durations, which is desirable for a DMS, as there may be long periods of inactivity.

For ITER applications, the temperature increase of the sabot is estimated to be quite small. Because of this, if the entire injector is maintained at cryogenic temperatures, the use of frozen neon or argon pellets may also be possible, and we note that rail guns have previously been proposed for fueling applications [25], but the use of these cryogenic materials is not considered at this time.

For near-term tokamak experiments, other radiative materials such as carbon or lithium, or a combination of materials, could also be used.

These would be injected into the plasma center for thermal and runaway electron mitigation. The radiative payload would be accelerated within 2 ms of the system trigger time, to the required velocities ~200–500 m s^{-1} for existing scale tokamaks, and to ~1 km s^{-1} or higher for ITER.

There are two important advantages of the EPI system. The first advantage of the EPI concept over gas-propelled injectors is its potential to meet the short warning time requirement. The system could also be located very close to the reactor vessel, which, in addition to substantially reducing the response time also improves the injector efficiency by beneficially utilizing the ambient magnetic fields that exist near a high-field tokamak, such as ITER. However, for the EPI system to be installed very close to the reactor vessel, it needs to be incorporated into the overall reactor design from an early stage. In this case, the entire injector would be mounted on rails, so that the entire assembly could be pulled back to a region of low radiation areas for maintenance. The reactor would likely have multiple DMS injectors, so that the DMS is always available. Because of the highly advanced state of the ITER design, this scenario is probably unlikely in ITER, so that an EPI system for ITER would likely be installed outside the port plug.

The second advantage has to do with impurity assimilation by the plasma. In the case of MGI and the shattered pellet system, the radiative payload material is deposited near the plasma edge, and relies on a complicated process for impurity assimilation, and mixing as described earlier [17]. Subsequent to the discharge assimilating a critical mass of impurities, the radiative collapse begins from the outer regions of the plasma and propagates inward.

With EPI, much of the needed radiative payload could be deposited in the core of the plasma where the runaway current channel originates. Thus, the amount of assimilated impurities is not governed by the pre-thermal quench physics. Additionally, the radiative payload from an EPI injection would trigger an inside-to-out thermal quench, such as that postulated for the shell pellet system. It should thus be much more suitable for suppressing the formation of a runaway current channel.

Again because of core deposition, much less radiative payload might be adequate for a more precise control of the thermal quench. Indeed, the theoretical work of Konavalov *et al* [26] suggests that as little as 5 g of Be may be adequate for both thermal quench and runaway electron mitigation in ITER. This radiative payload must be deposited deep in the plasma, and not at the edge as in present methods such as SPI. Clearly, more work on 3d MHD modeling of the plasma response to deep injection of low-*z* materials is needed to better define the requirements for ITER and to improve upon the early work of Konavalov.

Finally, because the EPI concept injects microspheres of known diameter and velocity one can precisely calculate the injection parameters needed for deep penetration in any plasma, including the ITER plasma. This makes it much easier to develop simulation capabilities that can be validated using present experiments and then used to reliably extrapolate to the needed requirements for ITER.

2.1. The EPI concept

As previously noted, the EPI system accelerates a metallic sabot to high velocity with an electromagnetic impeller, which releases a radiative payload, that is composed of low-*z* granules or a shell pellet containing smaller pellets.

Figure 1 describes the injector operating principle. The sabot is placed between two conducting rails separated by about 2–3 cm. The payload consisting of granules of a known size and size distribution, or a thin wall shell pellet containing the payload, is placed inside the hollow chamber of the sabot. A capacitor bank is connected to one end of the rails. Discharging the capacitor bank causes the current to flow along the rails as shown in figure 1. The $\mathbf{J} \times \mathbf{B}$ forces resulting from the magnetic field created in the region between the rails, and the current through the sabot accelerates the sabot and the payload. At the end of its acceleration, within 2 ms, the sabot is captured, and the payload is released.

The sabot would first be slowed down by using a wedged shaped assembly that is present between the rail muzzle and the entrance to a payload guide tube. This would have the effect of slowing down the sabot, which would allow the payload to separate from the sabot. After payload separation, a deflector plate would deflect the sabot along a different path—towards the sabot collection chamber. The vacuum chamber that encases the EPI system would retain the spent sabot. The spent sabot would be collected in a chamber located below the injector. On a periodic basis after numerous spent sabots have been collected these would be removed during routine maintenance of the injector.

The payload released by the sabot will then travel along a very shallow bend guide tube and be directed at some tangency to the plasma discharge so that in the absence of plasma, the payload material could impact a metallic tungsten armor that is positioned on the opposite wall along the injection direction. The tungsten armor would be designed to handle the full impact of the pellets and it would be similar in concept to the armor routinely used on tokamaks to absorb the neutral beam energy in the absence of plasma. In this case, the payload material would fall down on to the lower divertor region. The amount of payload material per shot is quite small compared to the amount of beryllium and tungsten used as plasma facing materials in ITER. On ITER any undesirable materials, whether they be the payload material, or melted plasma facing materials, if they should pose an issue for normal plasma operations could be removed by repeated plasma discharges designed to vaporize these materials.

Figure 1 shows the direction of the magnetic field generated by currents flowing along the rails. One way to increase the efficiency of the injector is to increase the magnetic field that penetrates the sabot region between the rails. This is because; the combination of the current flowing in the sabot and the magnetic field between the rails generates the accelerating $\mathbf{J} \times \mathbf{B}$ force. To increase this magnetic field, the ambient toroidal magnetic fields that exist near a high-field tokamak vessel, such as in ITER, could be used to augment the electrode-generated magnetic field by aligning the electrodes with the dominant external magnetic field. The benefits of this are described in [2]. For the case where the injector is located farther away from a reactor vessel (for example, outside the port plug of ITER), high-temperature super conducting (HTSC) magnets could be installed above and below the rails to increase the magnetic field to very high levels (8–12 T is possible with current technology [27]).

Adding this additional field has the advantage that a smaller power supply and a much lower level of rail current would be adequate to attain the same acceleration force. Thus, the large ambient magnetic fields near a tokamak vessel can help the EPI system improve its performance, and makes the system respond faster, by reducing the payload delivery time.

The velocities that can be achieved with the EPI can be calculated by solving the rail gun equations for a linear geometry and are described in [2]. Here, in figure 2, we present updated calculation results for an ITER-class EPI system that considers higher levels of magnetic fields permitted by recent developments in HTSC technology [28].

While in future reactor designs for which an EPI system could be a part of the initial integrated design where the EPI could be positioned very close to the reactor vessel, and therefore can benefit from the ambient magnetic field near the vessel, on ITER because the present design involves standardized port plugs, an EPI system either needs to be installed inside a port plug or just outside the port plug and a guide tube has to be used to transport the payload through the port plug into the ITER vessel.

Installation outside the port plug has the advantages that maintenance and even the replacement of an entire EPI injector would be readily accomplished. In addition, the external field augmentation can be increased to at least the 8 to 12 T range. Inside the port plug, one would use the ambient field present inside the port plug, but the response time would be faster due to the closer positioning of the injector to the vessel. Present discussions with ITER personnel has indicated that for a new system such as the EPI that was not part of the original ITER design, installation outside the port plug may be necessary, so we will consider this scenario and the improved performance possible with a field augmentation in the 8 to 12 T range.

Figure 2 shows acceleration parameters for 15 g mass, which is composed of an 8 g sabot plus 5 to 7 g payload. For cases A, B and C the rail generated field is augmented using external magnetic field producing coils. For comparison, a case without external field augmentation (Case D) is also shown. In figure 2, the ITER A case has 4 T augmentation; cases B and C have 8 and 12 T field augmentation respectively.

There are a number of important observations that can be made from the results. First, for a mass of 15 g, a 100 mF capacitor bank charged to between 0.85 to 2 kV accelerates the mass to about 1.3 km s^{-1} in about 2 ms. During this time
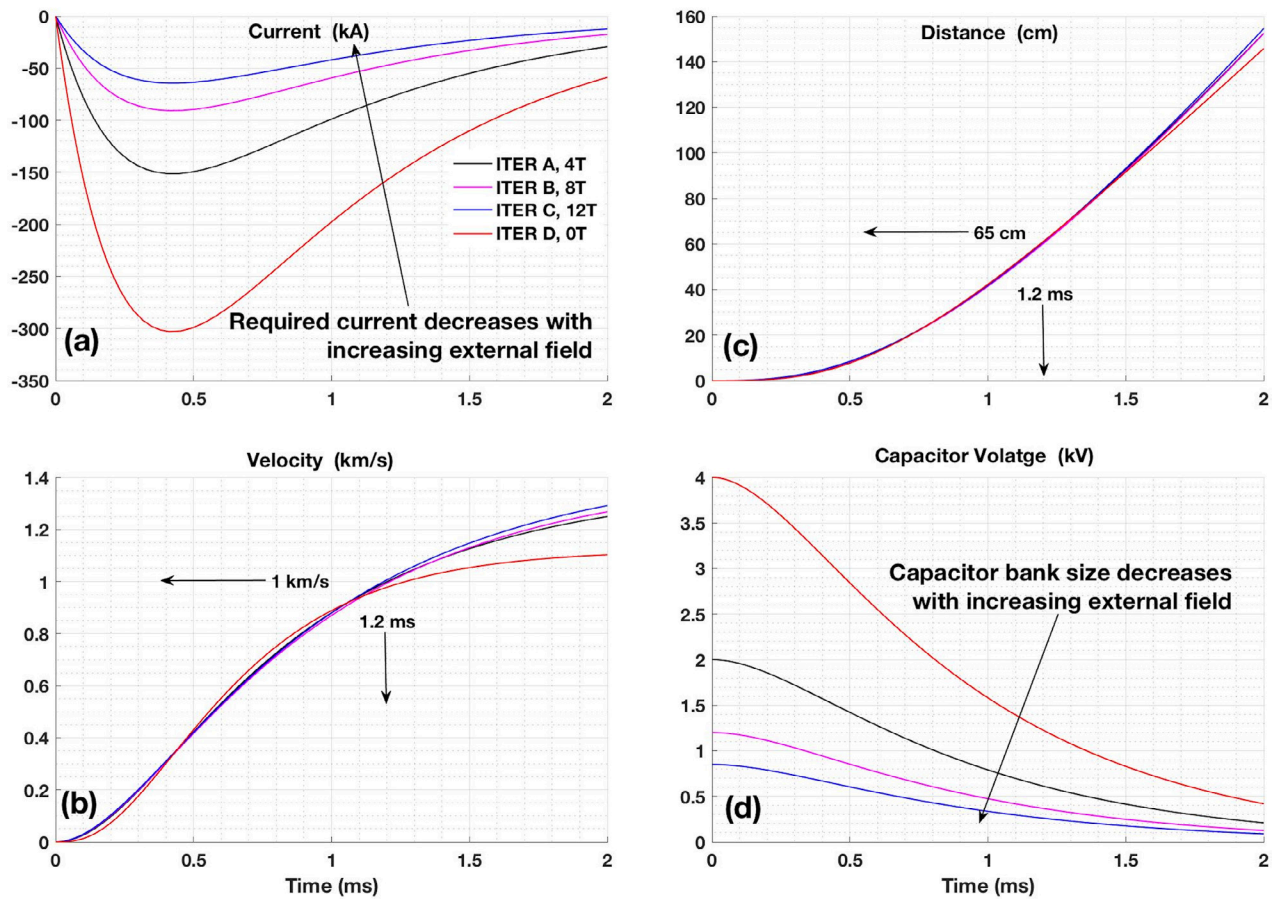
Figure 2. Calculations showing the capability of an ITER-class EPI system to accelerate a 15 g mass. Shown are four cases corresponding to an external magnetic field enhancement of 4 T, 8 T, 12 T, and 0 T. Shown are: (*a*) the current through the sabot, (*b*) attained accelerated velocities by the sabot, (*c*) the distance traveled by the sabot during the acceleration period, and (*d*) the initial charging voltage and the decrease in capacitor voltage during the acceleration phase.

duration, the projectile travels 1.5 m, so the accelerator length is 1.5 m for this operating scenario. Approximately 2 ms after the system is triggered, the accelerated payload traveling at 1.3 km s^{-1} therefore exits the injector.

As shown in figure 2, the dramatic reduction in the injector current, and the required operating voltage, for 8 and 12 T external magnetic field augmentation is seen for cases B and C, compared to the ITER 4 T case that has 4 T magnetic field assistance and the ITER 0 T case that has no field augmentation. At 8 T, a velocity of 1 km s^{-1} is attained at 1.2 ms at a charging voltage of just 1.2 kV, and the current reduces to just 80 kA. The lower current is highly desirable from the point of reducing electrode erosion and sabot heating. The bank energy is 70 kJ, which is only 75% higher than the size of the capacitor bank shown below in figure 3 that was used in a recent laboratory test of the concept reported in this manuscript.

With 12 T external magnetic field augmentation, which appears possible with recent developments in HTSC technology, the voltage and bank energy to attain 1 km s^{-1} in 1.2 ms is just 850 V and 40 kJ. This is the same as the bank energy used in present tests (figure 3) and the current through the sabot reduces to about 65 kA, which is 30% higher than the current level that was used to accelerate a 3.2 g sabot in the recent laboratory tests, which is described below.

The distance plot shows that an acceleration length of 1.5 m is needed to achieve velocities of 1.3 km s^{-1}. This is a relatively compact system. The capacitor voltage plot shows that most of the initial stored energy in the capacitor is depleted during the acceleration phase.

These calculated results suggest that the EPI concept has the potential to deliver the radiative payload on a fast time scale and with the high velocities needed for deep penetration into high power tokamak discharges. As a next step, it is highly desirable to know if small mass (few grams) sabots could indeed be accelerated to the required velocities on such a fast time scale. Section 3 describes such an experiment designed to test the response time of an EPI system.

We note that rail guns have been used in a number of fields including as a possible method for fueling using frozen fuel pellets [26]. A system that uses initial gas propulsion as the first stage of a railgun system has also been tested [29], and it has also been proposed for space launch applications [30]. But for all these applications, it is just the attainable high velocity that is important. It is not necessary for these systems to simultaneously respond on fast few milliseconds time scale as addressed in this manuscript. For the railgun to be viable as a DMS, both the fast time-response of the system and the attainable velocity are essential required parameters.
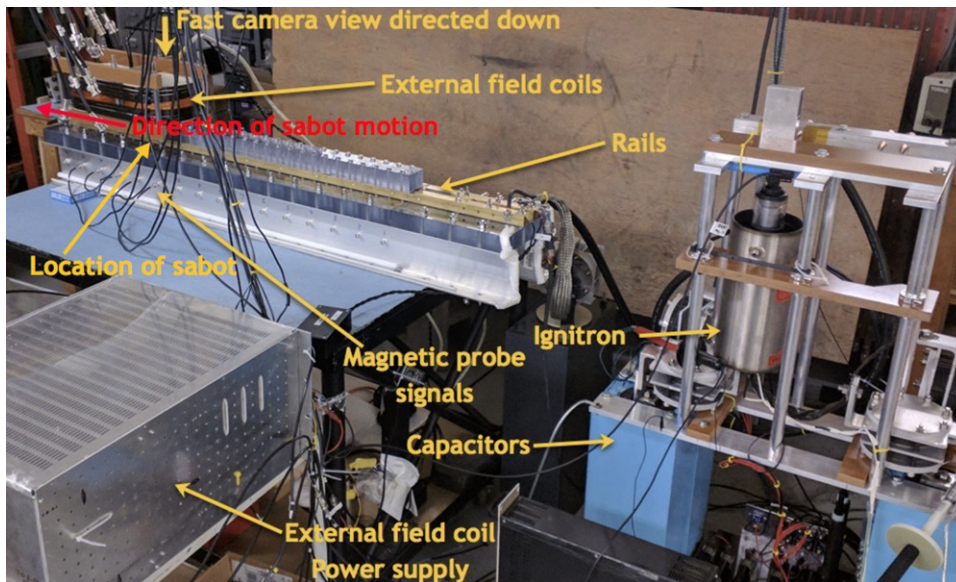
Figure 3. Experimental test setup used to verify the projected system response time and the attainable velocities. The system consists of 1 m long rails powered by a 20 mF, 2 kV capacitor bank triggered using a large size-D ignitron. Two circular magnetic coils placed above the rails provide an additional 30% magnetic field enhancement when the capacitor bank is operated at the full 2 kV capability. A separate capacitor bank (10 mF, 1.35 kV, switched by an SCR) is used to energize the external magnetic field coils.

3. Experimental results

To test if these very encouraging projections for an ITER scale injector are realistically achievable in a system that needs to accelerate few gram mass in a configuration compatible with an ITER DMS, a proto-type system was built at the University of Washington to test the attainment of the most important parameters that distinguishes the EPI's capabilities from conventional DM systems. These are the system response time and the attainable velocities on this fast time scale.

Figure 3 shows the main components of the experimental hardware. The system is composed of 1 m long rails, with a cross section of 2 cm × 2 cm and an electrode gap separation of 2 cm. Although calculations for this system indicated that the required acceleration length would be just 10–20 cm, the rails were made much longer to provide experimental flexibility and to factor in other possibilities that the simple model calculations may not have accounted for. One end of the rails is connected to a 20 mF, 2 kV capacitor bank. A 75 mOhm current limiting resistor is connected to each capacitor. The system is triggered using a single large size-D ignitron. A single, 2 m long, RG-218U coaxial cable was used to connect the capacitor bank to the rails. During tests, a sabot similar in shape to that shown in figure 1(*a*) (but without the cylindrical hollow chamber) was placed between the rails and the charged capacitor bank triggered.

It was found that initial tests in this configuration could not accelerate the sabot to velocities over 60 m s^{-1}. For this case, the calculated velocity was 80 m s^{-1}. The reason for this was attributed to some of the initial energy being depleted as there was insufficient force to rapidly accelerate the sabot during the initial current rise phase. Since the force on the sabot is proportional to the product of the current and the magnetic field, and with no external magnetic field present, this product is very small at the initial low current phase. For DMS

applications, it is necessary that the current rise be rapid (in order to minimize the acceleration time), so for these cases, the current needs to reach a threshold value before the sabot can move. Thus, some of the initial energy is wasted and does not contribute effectively to sabot acceleration. However, if some externally generated field is already present, then, the threshold current is lower and a much higher level of acceleration force is possible even at low rail currents. With this recognition, to increase the acceleration force during the initial current ramp-up phase, two circular magnetic field coils were installed on top of the rails, as shown in figure 3. These coils were powered by a 10 mF capacitor bank charged to 1.35 kV and were triggered using an SCR. The power supply we had built for operating massive gas injection (MGI) valves on NSTX-U were used to power these boost coils. Although these magnetic coils provide a field augmentation of just 30% of the peak rail generated fields, these were found to significantly improve the device performance; because this additional field, although small, is quite important as it allows the sabot to experience significant acceleration forces rapidly even during the initial rail current rising phase, and allows the sabot to gain velocity well before the rail generated currents reach high levels. When operated at the maximum permissible voltages, the externally generated boost field was 0.3 T and the rail generated fields at peak rail current was 1 T.

Magnetic probes located below the gap between the rails were used to track the motion of the sabot as the magnetic flux behind the sabot expands in time, propelling the sabot. An example of this data is shown in figure 4. The time variation of the peak in this signal on the different magnetic probes located along the injector can be used to calculate the velocity and the distance traveled.

A Phantom fast camera was mounted above the electrode gap. Optically transparent insulators were used to retain the electrodes in place so that fast camera observations could be
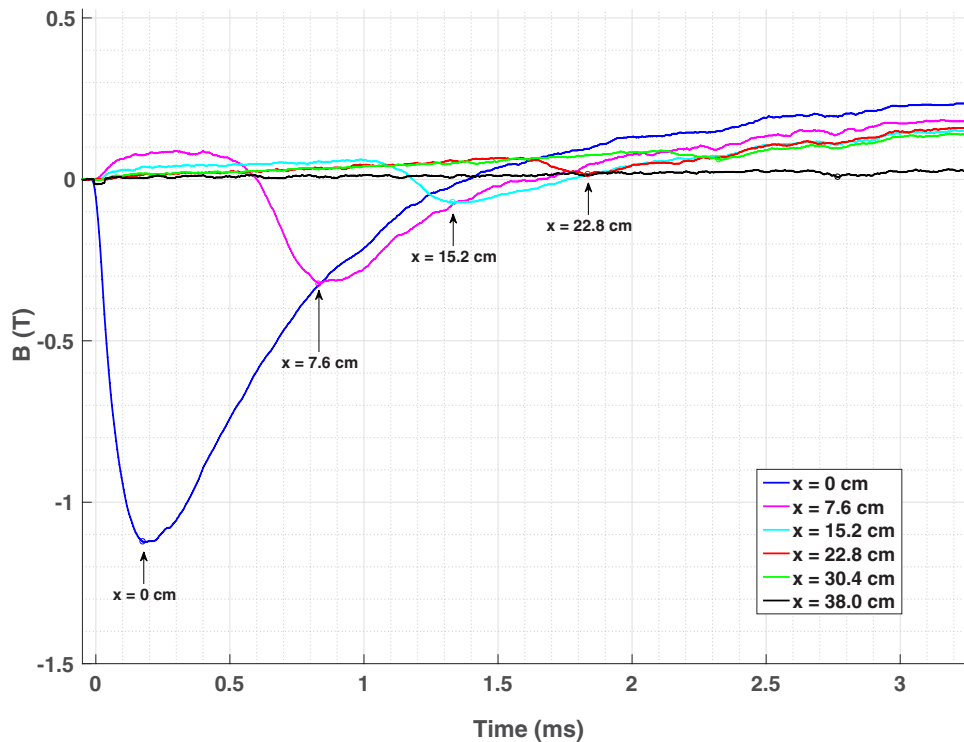
Figure 4. Traces from magnetic field pick-up probes located below the rail electrode gap. The probes respond to the expanding magnetic flux as the sabot travels past a probe. The signal from these probes can be used to calculate the velocity and the time response of the EPI system. The probes are separated by 7.6 cm from each other.

used to see the actual motion of the sabot. On an ITER scale injector, these would be replaced with high-quality alumina insulators. This measurement also allows one to calculate the velocity and the distance traveled by the sabot.

Figure 5 shows the reduced experimental data from figure 4 also augmented by the fast camera observations over plotted on the calculated values for this configuration. Figure 5 generally shows good agreement between the calculated and measured current through the sabot. The peak stored energy in the 20 mF capacitor bank was 40 kJ. The peak current through the sabot is 50 kA. The external coil located above the rails was also energized, and this provided an external field augmentation of 0.3 T (about 30% of the electrode generated fields). The sabot mass was 3.2 g. Figure 5(*b*) shows the sabot velocity evolution, where calculated values are compared to the measured values obtained using the fast camera data and from the magnetic probes (figure 4). The experimentally measured results from fast camera observation, and from the magnetic probes agree with the calculated velocity profile giving confidence that the concept can be extrapolated to attain higher velocities on the 1.5 to 2 ms time scale. Augmentation with higher levels of external field should further improve the concept, because the current driven though the system decreases dramatically, and thereby reduces the energy deposited in the sabot.

The results also show that the maximum velocity of 150 m s^{-1} that is obtained 1 ms after a command is issued to trigger the system, is consistent with the calculated values, verifying the rapid response capability of the EPI as a potential DMS. The calculations for the ITER case (figure 2) show that a

velocity of 1 km s^{-1} is achieved 1.2 ms after the system is triggered. For an injector positioned at the end of the ITER mid-plane port which has an overall length of about 4 m [31], the time taken for the payload to transit this distance and the additional 2 m minor radius of the ITER plasma is 6 ms. The overall system response time from time of trigger to reaching the plasma center is therefore 7.2 ms. The 1 km s^{-1} is by no means an absolute limit on the maximum velocity that could be attained by an ITER-class system and optimization at a higher velocity may be possible, which should further reduce the response time. Thus, the projected overall response time of <10 ms is a reasonable technically achievable estimate.

Note that this power supply with 40 kJ stored energy has about the same energy of an ITER-class system that would accelerate a 15 g mass to six times the velocity, but using 12 T field augmentation. Because of the very small size of the sabot, external magnetic field augmentation is particularly important for the application of this concept as a DMS. Future experiments should aim to increase the external field augmentation and conduct tokamak injection experiments in combination with simulations of low-*z* material penetration into tokamak plasmas. The radiative payloads should be composed of different elements and size to better define the near-term needs for an ITER DMS, to be considered as a backup concept for the SPI system.

In support of extrapolating this concept to facilitate a tokamak experiment, calculations for accelerating a 3.5 g sabot, containing 0.5 g of radiative payload to 500 m s^{-1}, indicate the need for a rail current of about 23 kA at 4 T. The operating voltage for this 20 mF system is just 1 kV, which is
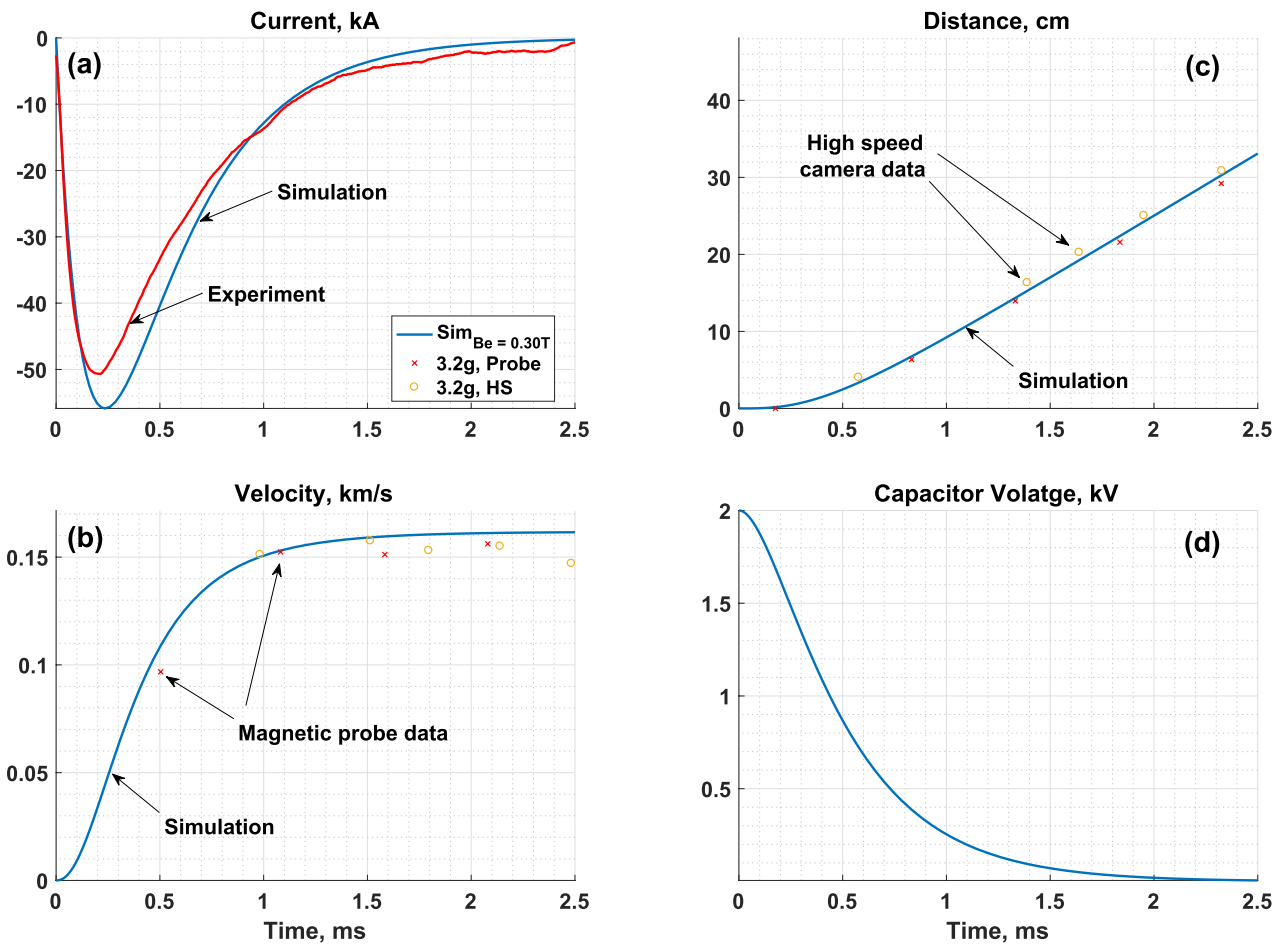
Figure 5. Comparison of the experimentally measured data with the calculated values for the setup shown in figure 3. The calculated values are shown by the blue traces. (*a*) The top-left traces show the measured (red) and the calculated (blue) rail currents, (*b*) the velocity as measured by the magnetic probes (shown as red crosses) and the velocity measured by the fast camera (shown by the yellow circles) and the calculated velocity trace (blue trace), (*c*) the distance traveled by the sabot during the acceleration period as measured by the magnetic probes (shown as red crosses), and by the fast camera (shown by the yellow circles), and the calculated distance trace (blue trace), and (*d*) the calculated capacitor bank voltage during the acceleration period.

much less than the 2 kV and 50 kA used in the EPI-1 experiments. If operated at the full 2 kV level, the attained velocity is 1 km s^{-1}, so in principle, the ITER/reactor relevant capability should be demonstrable with such a system.

Because the energy deposited in the sabot is proportional to the square of the current through the sabot, at these reduced currents of 23 kA, the temperature rise in the sabot is below 20 °C. At an ambient room temperature of about 22 °C, the sabot would reach a temperature of about 40 °C. The sabots are fabricated out of Al-7075-T6 material with the leading edges coated with tungsten. Aluminum is particularly good in this regard as it has low electrical resistivity and high specific heat (911 J/kg/K). Both these properties contribute to keeping the temperature rise in the sabot very low. For ITER applications, these sabots would be fabricated out of beryllium. Beryllium is much superior to aluminum. The specific heat of Be (1820 J/kg/K) is about twice that of aluminum, and the resistivity is lower than that of Al-7075. The resistivity of Al-7075-T6 is 52 nΩ m, while that for Be it is 36 nΩ m. This means that the sabot used on ITER can be much thicker, which would increase its heat capacity while further reducing its resistance. Unfortunately, due to safety regulations related to the use of

beryllium, the present phase of the EPI system cannot use beryllium sabots. Beryllium also has a much higher melting temperature (1287 C) compared to about 660 C for aluminum. This aspect, as well as the higher field augmentation that would be possible on a larger system, means that it should be technically much easier to extrapolate this concept to larger sizes.

4. Conclusions

The electromagnetic particle injector (EPI) is a novel fast time response disruption mitigation system that has a number of advantages over existing gas propelled systems and may be ideally suited for ITER applications. The EPI has the potential to deliver a low-*z* radiative payload to the plasma center on a <10 ms time scale, much faster, and deeper than what can be achieved using present methods. The EPI system accelerates a metallic sabot to high velocity using an electromagnetic impeller. At the end of its acceleration, within 2 ms, the sabot will release a radiative payload, which is composed of low-*z* granules of a known velocity and distribution, or a shell pellet containing smaller pellets. The primary advantage of the EPI

concept over gas propelled systems is its potential to meet short warning time scales, while accurately delivering the required particle size and materials at the velocities needed for achieving the required penetration depth in high power ITER discharges for thermal and runaway current mitigation. Experimental results from a proto-type system have accelerated a 3.2 g sabot to over 150 m s^{-1} within 1.0 ms, consistent with the calculations, giving confidence that larger systems could achieve the projected requirements of an ITER-scale injector. Since the EPI concept injects microspheres of known diameter and velocity one can precisely calculate the injection parameters needed for deep penetration into any plasma, including the ITER plasma. This makes is much easier to develop simulation capabilities that can be validated with present experiments and then used to reliably extrapolate to the needed requirements for ITER. Supporting theoretical simulations that can reliably extrapolate to ITER is essential to protect the integrity of the ITER facility.

As a next step, certain additional developments are needed and these need to be demonstrated in off-line tests before the design of an EPI system which could be considered for a tokamak installation.

First, it is necessary to show sabot-payload separation and the retainment of the sabot in the vacuum chamber used to house the EPI system. Second, it is also necessary to verify operation of the EPI system in vacuum. To demonstrate these capabilities, we are now developing a second-generation EPI system; the EPI-2 system. EPI-2 will operate with a boost field capability in excess of 2 T, which would permit studying the acceleration parameters as a function of externally applied magnetic field. EPI-2 will also be equipped with the payload separation, sabot capture system. During the first year, after an initial phase of operation in ambient atmosphere (to demonstrate sabot capture), it will be housed inside a vacuum chamber and operation under vacuum is planned for during the second year. The electrode life-time, reliability, and maximum achievable velocities will also be studied during this two-year research activity.

Mid-way during the second year, it is anticipated that sufficient knowledge will have been gained to permit the design of an EPI-3 system for deployment on a tokamak. It is anticipated that this system would operate at 3 to 4 T boost field. Other developmental aspects such as sabot loading under vacuum and directing the payload into a guide tube will be tested and incorporated in to the EPI built for a tokamak test. It is anticipated that the design and assembly of EPI-3 could be completed by the end of the third year. This would be followed by some off-line testing (during the fourth year) before deployment on a tokamak. Both DIII-D and KSTAR have expressed interest in testing the capability of an EPI as a DMS in support of ITER research.

Acknowledgments

ORCID iDs

R. Raman https://orcid.org/0000-0002-2027-3271
T.R. Jarboe https://orcid.org/0000-0001-7840-5524
J.E. Menard https://orcid.org/0000-0003-1292-3286

References

[1] Hollmann E.M. *et al* 2015 Status of research toward the ITER disruption mitigation system *Phys. Plasmas* **22** 021802

[2] Raman R. *et al* 2015 Fast time response electromagnetic disruption mitigation concept *Fusion Sci. Technol.* **68** 797

[3] Whyte D.G. *et al* 2003 Disruption mitigation with high pressure noble gas injection *J. Nucl. Mater.* **313–6** 1240

[4] Eidietis N.W. *et al* 2017 Poloidal radiation asymmetries during disruption mitigation by massive gas injection on the DIII-D tokamak *Phys. Plasmas* **24** 102504

[5] Pautasso G. *et al* 2009 Disruption studies in ASDEX Upgrade in view of ITER *Plasma Phys. Control. Fusion* **51** 124056

[6] Lehnen M. *et al* 2001 Disruption mitigation by massive gas injection in JET *Nucl. Fusion* **51** 123010

[7] Reux C. *et al* 2010 Experimental study of disruption mitigation using massive injection of noble gases on Tore Supra *Nucl. Fusion* **50** 095006

[8] Granetz R.S. *et al* 2007 Disruption mitigation studies on ALCATOR C-MOD and DIII-D *Nucl. Fusion* **47** 1086

[9] Bozhenkov S.A., Finken K.H., Lehnen M. and Wolf R.C. 2007 Main characteristics of the fast disruption mitigation valve *Rev. Sci. Instrum.* **78** 033503

[10] Finken K.H., Lehnen M. and Bozhenkov S.A. 2008 Gas flow analysis of a disruption mitigation valve (DMV) *Nucl. Fusion* **48** 115001

[11] Maruyama S. *et al* 2012 ITER fueling and glow discharge cleaning system overview *24th IAEA Fusion Energy Conf. (San Diego, USA, 8–13 October)* ITR/P5-24 (www-naweb.iaea.org/napc/physics/FEC/FEC2012/papers/332_ITRP524.pdf)

[12] Shiraki D. *et al* 2016 Thermal quench mitigation and current quench control by injection of mixed species shattered pellets in DIII-D *Phys. Plasmas* **23** 0625516

[13] Baylor L.R. *et al* 2010 Disruption mitigation technology concepts and implications for ITER *IEEE Trans. Plasma Sci.* **38** 419

[14] Baylor L.R. *et al* 2015 Disruption mitigation system developments and design for ITER *Fusion Sci. Technol.* **68** 211

[15] Lehnen M. 2017 *ITER Disruption Mitigation Workshop Report* ITER HQ ITER Organization

[16] Combs S.K. *et al* 1991 Repetitive two-stage light gas sun for high-speed pellet injection *Rev. Sci. Instrum.* **62** 1978

[17] Leonov V. *et al* 2014 Simulation of the pre-thermal quench stage of disruptions during massive gas injection and projections for ITER *Proc. IAEA-FEC 2014 Conf. (St. Petersburg, Russia, 13–18 October)* TH/P3-35 (www-naweb.iaea.org/napc/physics/FEC/FEC2014/fec2014-preprints/478_THP335.pdf)

[18] Parks P.B. and Wu W. 2014 Modeling penetration and plasma response of a dense plasma neutral gas jet in a post-thermal quenched plasma *Nucl. Fusion* **54** 023002

[19] Izzo V.A. 2006 A numerical investigation of the effects of impurity penetration depth on disruption mitigation by massive high-pressure gas jet *Nucl. Fusion* **46** 541

[20] Commaux N. *et al* 2010 Demonstration of rapid shutdown using large shattered deuterium pellet injection in DIII-D *Nucl. Fusion* **50** 112001

[21] Baylor L. 2017 Developments in shattered pellet technology and implementation on JET and ITER *PPPL TSD Workshop Report* Princeton Plasma Physics Laboratory (http://tsdw.pppl.gov/Talks/2017/Lexar/Monday%20Session%201/Baylor.pdf)

[22] Commaux N. *et al* 2016 First demonstration of rapid shutdown using neon shattered pellet injection for thermal quench mitigation on DIII-D *Nucl. Fusion* **56** 046007

[23] Snyder P.B. *et al* 2015 Super H-mode: theoretical prediction and initial observations of a new high performance regime for tokamak operation *Nuclear Fusion* **55** 083026

[24] Hollmann E.M. *et al* 2009 Low-*Z* shell pellet experiments on DIII-D *AIP Conf. Proc.* **1161** 65

[25] Onozuka M. *et al* 1997 High-speed hydrogen pellet acceleration using an electromagnetic railgun system *Fusion Eng. Des.* **36** 451–60

[26] Konovalov S.V. *et al* 2012 Studying the capabilities of Be pellet injection to mitigate ITER disruptions *Proc. IAEA-FEC 2012 Conf. (San Diego, USA, 8–13 October)* ITR/P1-38 (www-naweb.iaea.org/napc/physics/FEC/FEC2012/papers/338_ITRP138.pdf)

[27] Corato V. *et al* 2015 Detailed design of the large-bore 8T superconducting magnet for the NAFASSY test facility *Supercond. Sci. Technol.* **28** 034005

[28] Fietz W.H. *et al* 2016 High-current HTS cables: status and actual development *IEEE Trans. Appl. Supercond.* **26** 4800705

[29] Honig J. and Kim K. 1984 Pellet acceleration study with a railgun for magnetic fusion reactor refueling *J. Vac. Sci. Technol.* A **2** 641

[30] McNab I.R. 2003 Launch to space with an electromagnetic railgun *IEEE Trans. Magn.* **39** 295–304

[31] Lehnen M. 2015 Update on the ITER disruption mitigation system—physics basis and technology *PPPL TSD Workshop Report* Princeton Plasma Physics Laboratory (https://tsdw.pppl.gov/Talks/2015/13July15%20Theory%20and%20Simulations%20Workshop/Lehnen_TSDW2015.pdf)